

## A model for the release of sulfur from elemental S and superphosphate

Malcolm R. McCaskill<sup>1,2</sup> & Graeme J. Blair<sup>1</sup>

<sup>1</sup>*Department of Agronomy and Soil Science, University of New England, Armidale, N.S.W. 2351, Australia*

<sup>2</sup>*Present address: Division of Tropical Crops and Pastures, CSIRO, Private Mail Bag, PO Aitkenvale, Townsville, Qld. 4814, Australia*

Received 29 September 1988; Accepted in revised form 14 January 1989

**Key words:** Modelling, sulfur release

### Abstract

A mathematical model was developed to predict the release of sulfate from elemental S ( $S^0$ ) and gypsum in single superphosphate. The release algorithm is based on the observation that release is linearly related to particle surface area. Release rates under various conditions could then be described by the change in radius for each time increment, which allows easier comparison of release rates between different particle sizes. A model based on spherical particles was found to be adequate in accounting for the range of particle shapes found in crushed agricultural  $S^0$ . Release rates calculated from experimental data range from 0.07 to 0.45  $\mu\text{m}/\text{d}$  depending on environmental conditions.

Equations for incorporating the effects of environmental variables and the release of S from  $S^0$  and from the gypsum component of single superphosphate (SSP) were developed from the literature, and were incorporated within a larger model of S cycling. The model predicted that after 72 days, 99% of the S in SSP would have been released, compared to a release after one year of 54% of the S in sulfur-fortified superphosphate, and 23% of that in crushed agricultural grade  $S^0$ . The model provides a means of assessing the effect of the particle size of  $S^0$  on release rates and should allow the formulation of fertilizers that supply S at a rate closer to the rate of plant uptake.

### Introduction

Elemental sulfur ( $S^0$ ) is a component of most commercially available fertilizers with an analysis > 26% sulfur (S). It is insoluble in water and oxidized to plant-available forms by microorganisms which use the exothermic oxidation reaction for their metabolic activity. Its rate of oxidation is affected by soil temperature, soil moisture, the  $S^0$ -oxidizing biota present, and the exposed surface area of  $S^0$  available for microbial attack. Some control of  $S^0$  release rate is possible by altering particle size. This potential makes it possible to more closely match the release rate with plant requirements, so as to minimize sulfate leaching. There have been numerous trials comparing various particle sizes under incubation, pot and field

conditions [e.g. 1, 6, 9, 11, 12, 17, 18, 19], but only a few have been monitored for two years or more. Fox and coworkers [6] found a linear relationship between  $S^0$  release over an initial 30 day period and surface area, where surface area was calculated assuming particles were spheres with a diameter equal to the sieve size. While adequate to explain particle size differences during the initial release period in all the reports cited above, this theory has not yet been extended to describe release over a longer time period.

Sulfate fertilizers such as gypsum and superphosphate are also released at a rate dependent upon their particle size, and theory developed for  $S^0$  should also be applicable to these materials. This paper describes the development of a model for the long-term release of  $S^0$  in response to climatic varia-

bles, and its extension to describe the release of S from superphosphate.

## Model development

### A simple model

The theory that release is linearly related to surface area, when surface area is calculated by assuming the particles are spheres, can be developed into a simple model to predict the changes in release characteristics which would be expected over time. Standard mathematical equations are available for calculating the area (A) and mass (M) of a sphere from its radius (r) and density ( $\rho$ )

$$A = 4\pi r^2 \quad (1)$$

$$M = \rho \frac{4}{3}\pi r^3 \quad (2)$$

where  $\rho = 2 \text{ kg/L}$  or  $2 \text{ ng/mm}^3$

Release from the particle on day t ( $R_t$ ) is then the product of the area and the release per unit surface area ( $R_A$ )

$$R_t = R_A A \quad (3)$$

This equation is exact if the object is completely flat, but slightly overestimates release from convex objects. The new particle radius at time t can then be calculated by subtracting  $R_t$  from M, using the appropriate subscripts within a rearrangement of equation (2):

$$r_t = \sqrt[3]{\frac{M_{t-1} - R_t}{\rho \frac{4}{3}\pi}} \quad (4)$$

Equations (3) and (4) were used to illustrate the relationship between  $r_t$ ,  $R_t$  and specific surface area (SSA) for a particle with an initial diameter of 0.183 mm oxidizing at a rate per unit area ( $R_A$ ) of 0.004 kg  $S^0$ /m<sup>2</sup>/d. Predictions from this simulation (Fig. 1) show that  $R_t$  and SSA changed with time according to curvilinear relationships, while  $r_t$  fell at a virtually constant rate. The rate at which the radius decreased ( $\Delta r$ ) remained constant until the particle had reached a very small size. The only factor to destroy the constant relationship between  $R_A$  and  $\Delta r$  was the error in equation (3), which becomes more significant for small particles and with larger timesteps, as illustrated in Fig. 1. The error in this equation also affected the time to

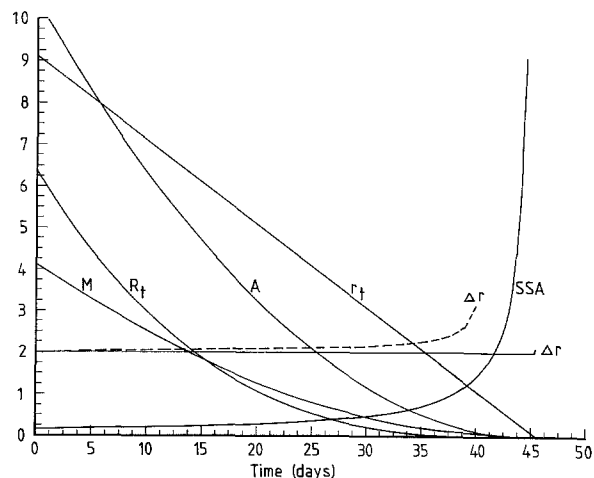


Fig. 1. Relationship between particle radius ( $r_t$ ,  $m \times 10^{-5}$ ), mass (M,  $kg \times 10^{-9}$ ), area (A,  $m^2 \times 10^{-8}$ ), specific surface area (SSA,  $m^2/kg \times 10^{-2}$ ), release ( $R_t$ ,  $kg/d \times 10^{-10}$ ) and change in radius ( $\Delta r$ ,  $m/d \times 10^{-6}$ ), as calculated from equations (3) and (4) with a timestep of 0.001 d (solid lines), and  $\Delta r$  with a timestep of 1 d (dashed line).

complete release of the particle, from 40 d with a timestep of 1 d, to 44.4 d with a timestep of 0.001 d.

In most investigations of  $S^0$  release [5, 6, 9, 10, 12, 16, 18, 19] oxidation rate has been measured by the rate of appearance into the sulfate form—an approximation of  $R_t$ . Since  $R_t$  varies even under constant oxidation conditions, it would be preferable to specify release rates in terms of  $R_A$  or  $\Delta r$ . Of these two parameters, the model based upon the use of  $R_A$  yielded predictions which were sensitive to timestep, and it was considered preferable to redefine to model into a form which is independent of timestep, based instead upon  $\Delta r$ . Release can then be described by an exfoliation principle in which the particle radius is reduced by a constant amount in each timestep. Particle radius at time t ( $r_t$ ) can then be calculated from its previous radius ( $r_{t-1}$ ) as

$$r_t = r_{t-1} - \Delta r \quad (5)$$

and  $R_t$  as

$$\begin{aligned} R_t &= (\text{previous particle mass} - \text{current particle mass})/\text{timestep} \\ &= (\rho \frac{4}{3}\pi r_{t-1}^3 - \rho \frac{4}{3}\pi r_t^3)/\Delta t \end{aligned} \quad (6)$$

### Detailed examination of sulfur particles

Although the spherical particle model was ade-

quate for explaining particle size differences in the work of Fox et al. [6], there are no reports in the literature of the particle shapes of crushed  $S^0$ . Particles of yellow recovered  $S^0$  prepared in a commercial roller crusher were examined in three ways— (i) by surface area measurement using the standard BET method [3], (ii) by visual measurement of 100 particles in the 1 mm sieving fraction, and (iii) by electron microscopy of particles before and after 22 and 34 months of exposure to soil in a grazing experiment [13].

Attempts to measure surface areas by the BET method were unsuccessful because of particle porosity and  $S^0$  volatilization at the low pressures used in the technique. Visual measurement was more successful. Mean length was 1.43 mm, breadth 1.07 mm and thickness 0.63 mm, with standard deviations of 0.412, 0.202, and 0.232 mm respectively. Variation in each dimension fitted criteria for a Normal distribution. A sizeable proportion of particles were tetrahedral in shape with all three dimensions close to 1.0 mm. Electron micrographs showed smooth shear planes on unexposed particles, but surface pitting on exposed particles (Fig. 2), suggesting a mechanism whereby the surface area could increase with time.

#### Spheroidal particle model

Since the particles were clearly not spheres, a spheroidal particle model was used for comparison with

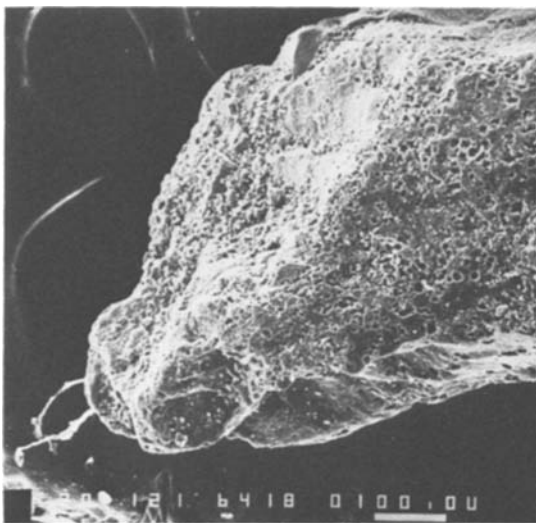


Fig. 2. Electron micrograph of a typical  $S^0$  particle after at least 18 months of field exposure. Magnification  $200\times$ .

the spherical model presented earlier. The 100 length, breadth and thickness measurements were converted to a, b and c axis lengths (analogous to the radius of sphere) for use within the following routine to calculate  $R_t$  by an adaptation of equations (5) and (6):

$$a_t = a_{t-1} - \Delta r$$

$$b_t = b_{t-1} - \Delta r$$

$$c_t = c_{t-1} - \Delta r$$

$$R_t = \rho \frac{4}{3}\pi(a_{t-1} \cdot b_{t-1} \cdot c_{t-1} - a_t \cdot b_t \cdot c_t) \quad (7)$$

For comparison between spheroidal and spherical models, the same shapes were assumed for particles 0.1, 0.4 and 2.0 mm in diameter. Figure 3a shows that for the same value of  $\Delta r$  ( $0.2 \mu\text{m}/\text{d}$ ), the spheroidal model predicted more rapid release than the spherical model. To compensate,  $\Delta r$  in the spherical model was increased iteratively until its release pattern was as close as possible to that of the spherical model. Figure 3b shows that an extremely close fit could be achieved by a 12% increase in  $\Delta r$ . The spherical particle model is

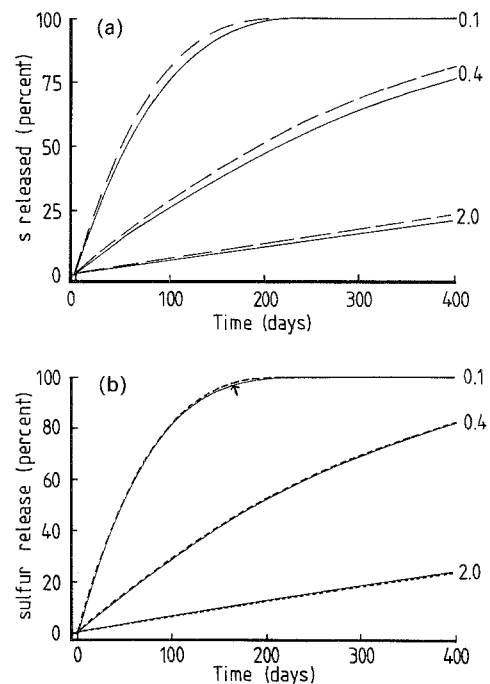


Fig. 3. Cumulative  $S^0$  release as calculated by the spherical (solid lines) and spheroidal (dashed) particle models for particles with initial diameters of 0.1, 0.4 and 2.0 mm. (a) Both models,  $\Delta r = 0.2 \mu\text{m}/\text{d}$ ; (b)  $\Delta r$  for the spherical model increased by 12% to  $0.224 \mu\text{m}/\text{d}$ .

therefore a simpler alternative to its spheroidal counterpart, provided it is realized that values of  $\Delta r$  calculated for use in the spherical model are higher than could be measured on actual particles.

#### Derivation of $\Delta r$ from experimental data

For use in the spherical particle model,  $\Delta r$  can be calculated from experiments where particles of a known diameter ( $d$ , mm) have been added to soil, and where the  $S^0$  remaining after  $t$  days has been extracted by chloroform [1] or acetone [4, 15, 17]. Since the proportion of added  $S^0$  remaining in the elemental form ( $E_t$ , dimensionless) after  $t$  days is the fraction (current mass)/(initial mass), this can be expanded to

$$E_t = 4/3\pi r_t^3 \rho N / (4/3\pi r_0^3 \rho N) \quad (8)$$

where  $r_0$  (mm) is the initial radius,  $r_t$  (mm) the radius after  $t$  days, and  $N$  the number of particles

applied. By cancelling and rearrangement,

$$r_t = r_0 \sqrt[3]{E_t} \quad (9)$$

as  $\Delta r$  expressed as

$$\Delta r = (r_0 - r_t)/t \quad (10)$$

or by substituting  $r_t$  from (9),

$$\Delta r = (d/2)(1 - \sqrt[3]{E_t})/t \quad (11)$$

Release rates calculated from the literature by equation (11) range from about 0.1 to 0.4  $\mu\text{m}/\text{d}$  depending on environmental conditions (Tables 1 and 2). There is no evidence for an increase in  $\Delta r$  with time, despite the pitting effect noted in the electron micrograph (Fig. 2). Release rates for the dark Frasch  $S^0$  are slightly higher than for the more common bright yellow  $S^0$  recovered from sour gas wells. Other work [13] has shown that for the same sieving fraction, dark  $S^0$  is released 30% faster than bright  $S^0$ , because dark particles within the sieving fraction are actually agglomerates of smaller particles.

Table 1. Summary of release rates calculated from experiments in which  $S^0$  oxidation rates were determined by analysis of residual  $S^0$

Reference no.	Overall conditions	Treatment conditions <sup>+</sup>	Mean release ( $\mu\text{m}/\text{d}$ )
[1]	Field; 5–35°C; bright $S^0$ ; 0.07–0.44 mm diam.; 66 kg/ha; samplings between 10 and 510 d	Wet site Drier site	0.148 0.096
[4]	Incubated; 25–35°C; bright $S^0$ ; < 0.2 mm diam.; 320–8000 kg/ha; samplings between 7 and 49 d	Sandy loam Clay loam	0.190 0.127
[17]	Glasshouse; –6–28°C; dark $S^0$ ; 0.05–1.00 mm; 2–1750 kg/ha; 140 d	15*kg/ha 29*kg/ha 117*kg/ha	0.359 0.129 0.129
[17]	Growth cabinet; 18–30°C; dark $S^0$ ; 0.1–0.4 mm; 55 kg/ha; 168 d	0.1 mm 0.4 mm	0.202 0.335

<sup>+</sup> Mean release rates are presented for some of the treatments tested.

\* These application rates refer to the 0.1 mm size. Application rates for other sizes were equivalent on a surface area basis (assuming spherical particles).

Table 2. Release rates calculated from the experiment of McCaskill and Blair [14] for bright  $S^0$  under glasshouse conditions

Size (mm diameter)	Inoculation	Soil clay content (%)				5% LSD
		9.3	21.8	45.3	52.3	
0.2	–	0.266	0.206	0.292	0.210	0.022
	+	0.307	0.271	0.291	0.255	
0.4	–	0.314	0.211	0.425	0.258	0.049
	+	0.399	0.361	0.453	0.357	
1.0	–	0.094	0.073	0.264	0.108	0.075
	+	0.757	0.232	0.353	0.258	

Table 2 shows significant differences in  $\Delta r$  among 0.2, 0.4 and 1.0 mm particle sizes, with release rates for both 1.0 mm and 0.2 mm sizes lower than for the 0.4 mm size. The 1.0 mm size had a lower mean release rate because of slower oxidation rates on soils lacking rapid  $S^0$ -oxidisers such as *Thiobacillus thiooxidans*. Differences in oxidation rate because of differences in  $S^0$ -oxidising organisms become more evident in particles  $> 0.4$  mm [14]. Release rates from the 0.2 mm size were lower because the spherical model overestimates cumulative release relative to its spheroidal counterpart when only a small proportion of the initial  $S^0$  remains in the sample (arrow, Fig. 3b), leading to an underestimate of  $\Delta r$ .

#### Incorporation of environmental variables

For predicting the release of  $S^0$  under field conditions in larger nutrient cycling models such as that outlined by McCaskill and Blair [15],  $\Delta r$  for each days simulation can be calculated from a maximum release rate,  $\Delta r_{\max}$  and the product of scalars to account for below-optimal temperature ( $f_T$ ) and moisture ( $f_\theta$ ) conditions:

$$\Delta r = \Delta r_{\max} \cdot f_T \cdot f_\theta \quad (12)$$

Additional scalars would be required to account for the application rate effect which is sometimes observed at application rates greater than those normally required for correcting S deficiencies [17], and when particles  $> 0.5$  mm comprise a substantial portion of the fertilizer S [14]. Under both these conditions, release rates are likely to be reduced if  $S^0$  oxidation relies on heterotrophic soil organisms, but reductions are less likely if acid-tolerant  $S^0$  oxidisers such as *Thiobacillus thiooxidans* are present.

$f_T$ : Microbial oxidation of sulfur proceeds very slowly at temperatures of 4°C, and increases as a linear function of temperature until 35°C [4, 5, 7, 12, 17]. Expressed mathematically,

$$f_T = \max(0, -0.103 + 0.0315T_s); \quad f_T \leq 1.0 \quad (13)$$

where  $T_s$ (C) is the soil temperature.

$f_\theta$ : Soil moisture contents of 90% maximum water-holding capacity are optimal for sulfur oxidation

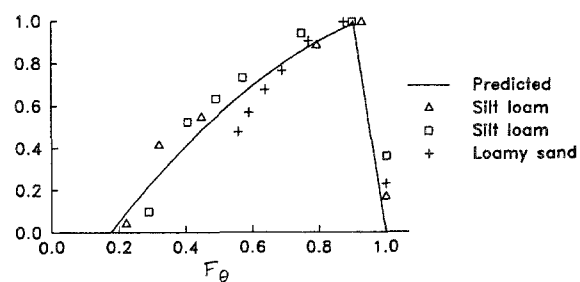


Fig. 4. Effect of soil moisture on  $S^0$  oxidation rate [16], and  $f_\theta$  as calculated by equation [14].

[5, 11, 16]. Oxidation rates decrease at higher moisture contents due to poor aeration, and at low moisture contents because a smaller proportion of exposed  $S^0$  would be covered by a water film. A relationship derived by regression from the data of Moser and Olsen [16], shown in Fig. 4, can be represented as

$$f_\theta = -0.386 + 2.37F_\theta - 0.945(F_\theta)^2; \quad (14)$$

$$r^2 = 0.913$$

for fractional soil moisture contents ( $F_\theta$ , (current volumetric soil moisture)/(volumetric soil moisture at field capacity)) ranging from 0.0 to 0.9, and  $f_\theta = 10 - 10F_\theta$  for  $F_\theta$  between 0.9 and 1.0.

#### Sulfate release from single superphosphate

Single superphosphate consists of a mixture of calcium phosphate and gypsum. Water-soluble phosphate diffuses from the superphosphate granule about 50 times faster than the sulfate, leaving a shell of gypsum and sparingly soluble phosphates [21, 22, 23]. Release of the residual sulfate is a linear function of surface area [Note 1] and linearly related to  $F_\theta$  [Note 2]. S dissolution is also increased by leaching, 100 mm of rainfall causing the release of 50% of S from a 5.6 mm particle [21]. From equation (11), this is equivalent to 5.78  $\mu\text{m}$  for each millimeter of rainfall, and 1.65 times the value of 3.50  $\mu\text{m}/\text{d}$  for moist soil conditions without leaching. Dissolution of the S component of superphosphate can therefore be modelled by equations (5) and (6) with  $\Delta r$  calculated as

$$\Delta r = \Delta r_{\max} F_\theta + 1.65 \Delta r_{\max} r_{\text{mm}} \quad (15)$$

where  $\Delta r_{\max}$  is the maximum daily release rate with-

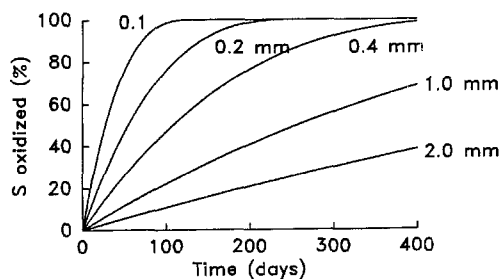


Fig. 5. Release pattern predicted for  $S^0$  by equations (5) and (6) for a release rate of  $0.4 \mu\text{m/d}$  and particles with initial diameters of 0.1, 0.2, 0.4, 1.0 and 2.0 mm.

out leaching, equal to  $3.5 \mu\text{m/d}$ , and  $r_{\text{mm}}$  (mm) the day's rainfall.

### Predictions

The release pattern predicted for a range of discrete particle sizes with a constant release rate of  $0.4 \mu\text{m/d}$  is shown in Fig. 5. For the sizes shown, particles  $<0.5$  mm diameter were almost completely released after one year, but the larger particles still contained 40% of their S in the elemental form. The difference between particles less than and greater than 0.5 mm diameter is likely to be greater than that shown in Fig. 5, because of the effects of

$S^0$ -oxidizing biota which become evident between 0.4 and 1.0 mm diameter (Table 2), and because of a rounder shape in 2.0 mm particles [14].

Commercially available fertilizers contain a range of particle sizes rather than discrete sizes. To simulate these, a range of representative initial diameters was used along with sieve analysis information [13] for (i) agricultural grade crushed  $S^0$ , as available commercially in Australia, (ii) sulfur-fortified superphosphate (SF45), in which finely divided  $S^0$  is incorporated within superphosphate granules and (iii) the S contained in single superphosphate (SSP). Maximum release rates ( $\Delta r_{\text{max}}$ ) chosen for  $S^0$  were 0.4, 0.3 and  $0.2 \mu\text{m/d}$  for particle sizes 0–0.5, 0.5–1.0, and 1.0 mm respectively. Release patterns predicted by these relationships within a larger nutrient cycling model [15] for S applied to a grazing experiment [17] at Armidale, N.S.W. on August 30, 1979 (Fig. 6) shows relatively rapid release of the sulfate-S contained in SSP, and more gradual release of the  $S^0$ , even within the finest particle size fraction. Release rates of  $S^0$  were lower during periods when the topsoil was dry, and when soil temperatures were low during winter. These periods of slow release coincide with periods when plant demand for S would also be low. After 72 days, 99% of SSP had been released, but after one year, only 54% of the S in SF45 had been

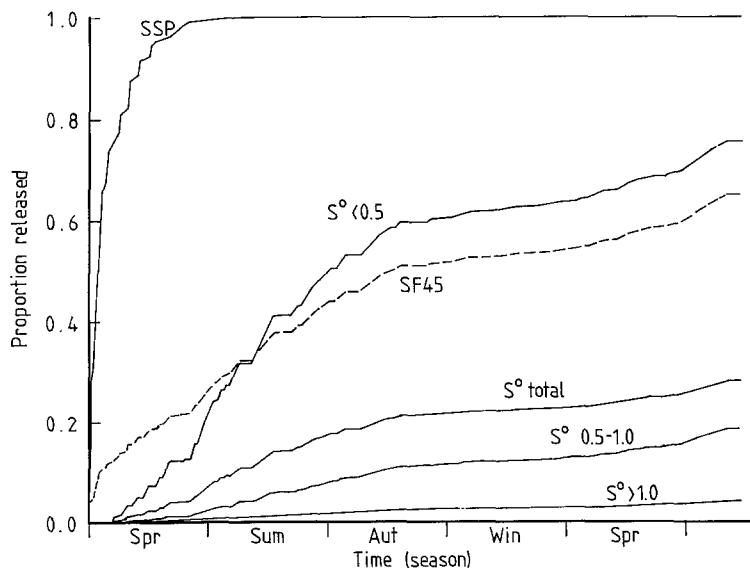


Fig. 6. Release pattern predicted by equations (5), (6), and (12)–(15) for various S fertilizers applied to a grazing trial [17] at Armidale, N.S.W. SSP: Single superphosphate; SF45: sulfur-fortified superphosphate;  $S^0$ : agricultural grade crushed  $S^0$  (total), and size fractions within it of  $<0.5$ , 0.5–1.0 and  $>1.0$  mm diameter.

released, and 23% of the crushed  $S^0$ . Within the crushed  $S^0$ , 64% of the 0.0–0.5 mm fraction had been released, compared with 13% and 3% respectively for the 0.5–1.0 and 1.0 mm fractions. These simulations illustrate a conclusion from many field trials (see [14]), that  $S^0$  particles with a diameter greater than about 0.5 mm release at such a slow rate as to be not useful over an economic timespan. Since agricultural grade crushed  $S^0$  is, because of aviation safety requirements, required to carry a large proportion of its mass as particles  $> 0.5$  mm, it is preferable to utilize other products such as SF45 to correct S deficiencies. If a rapidly-released product is required with a higher S analysis, the incorporation of  $> 10\%$  sodium bentonite within  $S^0$  prills has been shown to disperse to a material in which virtually all its  $S^0$  particles are  $< 0.5$  mm in diameter [2].

### Conclusions

The model as presented is an integration of what is currently known about the release of sulfate from  $S^0$  and SSP. Because no reliable validation data were available, it was not possible to independently test the accuracy of the predictions under field conditions. For many purposes, the extra cost involved in more thorough validation would not be justified, since conclusions from the model are in general agreement with those from past field trials. Even without thorough validation of release rates under various conditions, the model parameter  $\Delta r$  provides a powerful means of expressing release rates, which can be easily used to predict release patterns for slow-release fertilizer materials, and allow comparison of a range of possible particle size compositions.

### Acknowledgments

We thank the Australian Wool Corporation for providing funding for this research from its Wool Research Trust fund, and appreciated the assistance of Miss Alice Lav and Dr. Franz Grieser of the University of Melbourne for attempting the BET surface area measurements of  $S^0$  particles.

### Notes

1. Linear correlation coefficient ( $r^2$ ) between S released and  $1/r_0$  (proportional to the initial surface area) was 0.98 for data in Table 6, in reference [20], and 0.96 for Fig. 7a in reference [22].
2. Linear correlation coefficient ( $r^2$ ) between total S released into a hemisphere around the granule and  $F_\theta$  was 0.98 for data read from Fig. 7b in reference [20].

### References

1. Barrow NJ (1971) Slowly available fertilizers in southwestern Australia. 1. Elemental sulfur. *Aust J Exp Agric Anim Husb* 11: 211–216
2. Boswell CC, Owers WR, Swanney B and Rothbaum HP (1988) Sulfur/sodium bentonite mixtures as sulfur fertilizers. 1. The effects of S/Na-bentonite ratios on the rate of dispersion and particle size distribution of elemental sulfur dispersed from laboratory-produced prills. *Fert Res* 15: 13–31
3. Brunauer S, Emmett PH and Teller E (1938) Adsorption of gases in multimolecular layers. *J Am Chem Soc* 59: 309–319
4. Chopra SL and Kanwa JS (1968) Effect of some factors on the transformation of elemental sulfur in soils. *Indian Soc Soil Sci J* 16: 83–88
5. Fawzi Abed, MAH (1976) Rate of elemental sulfur oxidation in some soils of Egypt as affected by the salinity level, moisture content, temperature and inoculation. *Beitr Trop Landwirtschaft Veterinarmed* 14: 179–185
6. Fox RL, Atelsalp HM, Kampbell DH and Rhoades HF (1964a) Factors influencing the availability of sulfur fertilizers to alfalfa and corn. *Proc Soil Sci Soc Am* 28: 406–408
7. Fox RL, Flowerday AD, Hosterman FW, Rhoades HF and Olson RA (1964b) Sulfur fertilizers for alfalfa production in Nebraska. *Nebraska Agric Exp Sta Bull* No 214
8. Hutchinson KJ and Roper MM (1985) The importance of plant and animal residues in the nutrient economies of pasture and cropping systems. In: R.A. Leng et al., (eds). *Reviews in Rural Science*, 6, 207–218. Biotechnology and recombinant DNA technology in the animal production industries. Armidale: University of New England
9. Jones MN and Ruckman JE (1969) Effect of particle size on long-term availability of sulfur on annual-type grasslands. *Agron J* 61: 936–939
10. Keimnec G, Jackson TLK and Mosher W (1981) Fertilizing subclover with elemental sulfur. *Sulfur in Agric* 5: 12–16
11. Kittims HA and Attoe OJ (1965) Availability of phosphorus in rock phosphate-sulfur fusions. *Agron J* 57: 331–334
12. Li P and Caldwell AC (1966) The oxidation of elemental sulfur in soil. *Proc Soil Sci Am* 30: 370–372

13. McCaskill MR (1984) The residual effects of elemental sulfur as a pasture fertilizer. M Ru Sci Thesis. Armidale: University of New England
14. McCaskill MR and Blair GJ (1987) Particle size and soil texture effects on elemental sulfur oxidation. *Agron J* 79(6): 1079–1083
15. McCaskill MR and Blair GJ (1988) Development of a simulation model of sulfur cycling in grazed pastures. *Biogeochem* 5: 165–181
16. Moser US and Olson RV (1953) Sulfur oxidation in four soils as influenced by soil moisture tension and sulfur bacteria. *Soil Sci* 76: 251–256
17. Shedley CD (1982) An evaluation of elemental sulfur as a pasture fertilizer. PhD Thesis. Armidale: University of New England
18. Spencer K (1968) Availability to clover of sulfur as gypsum and brimstone of different particle sizes. *Fld Stn Rec, Aust. CSIRO Div. Plant Industry* 7: 1–12
19. Weir RG, Barkus B and Atkinson WT (1963) The effect of particle size on the availability of brimstone sulfur to white clover. *Aust J Exp Agric Anim Husb* 3: 314–318
20. Williams CH (1969) Moisture uptake by surface-applied superphosphate and movement of the phosphate and sulfate into the soil. *Aust J Soil Res* 7: 307–316
21. Williams CH (1971a) Reaction of surface-applied superphosphate with soil. 1. The fertilizer solution and its initial reaction with soil. *Aust J Soil Res* 9: 83–94
22. Williams CH (1971b) Reaction of surface-applied superphosphate with soil. 2. Movement of the phosphorus and sulfur into the soil. *Aust J Soil Res* 9: 95–106